Transactions of the Materials Research Society of Japan 25 [4] 995-998 (2000)

Photoionization and photodissociation studies of semiconductor clusters

Shinji Yoshida and Kiyokazu Fuke*
Department of Chemistry, Kobe University, 1-1 Nada-ku, Kobe 657-8501 Japan
*Fax: 078-803-5673, e-mail: fuke@kobe-u.ac.jp

Photoionization thresholds for Ge_n ($n \leq 57$) and Sn_n ($n \leq 41$) are investigated with detection by reflectron time-of-flight mass spectrometry. Stimulated Raman scattering lights of narrow bandwidth UV radiation are used as the ionization light source in the vacuum ultraviolet region (200-141 nm). A very similar size dependence of ionization potentials (IPs) is found for Ge_n and Sn_n with less than 12 atoms. We also find a rapid decrease in IPs for Ge_n between n=15 and 26, which is similar to that for Si_n found in our previous work. On the other hand, the IPs of Sn_n (n=15-41), which is metallic in bulk solid at room temperature, are found to decrease slowly without a gap. The difference in the size dependence of IPs for the medium size Si_n, Ge_n, and Sn_n clusters is discussed in relation to the existence of a structural transition. We have also examined the photodissociation process of Sn_n^+ clusters. We observe a trend for the evaporation of atom and/or dimer, which is usually observed for metal clusters, in addition to a fission-type fragmentation as is observed for Si_n^+ and Ge_n^+.
Key words: photodissociation, ionization potential, germanium, tin, cluster

Introduction

The physical and chemical properties for the clusters of group 14 elements have been investigated intensively for the last decade because of their importance both in fundamental and applied science. For example, several groups have studied the photodissociation and collision-induced dissociation (CID) processes of Si_n and Ge_n to gain information on the stabilities and binding energies of these clusters.[1-3] The vibrational frequencies of small Si_n clusters have been also investigated by various spectroscopic methods.[3] Recently, Jarrold and co-workers have measured the mobilities of Si_n^+, Ge_n^+, and Sn_n^+ using injected-ion drift-tube techniques to obtain information on the structures of these clusters. As for Si_n^+, they have found the existence of isomers having different mobilities: they have suggested the occurrence of structural transition between these isomers. Although these experimental studies afford information on the global structure of clusters, most of the structural data come from the theoretical calculations. In order to determine the most stable geometries and electronic structures of Si, Ge, and Sn clusters, numerous theoretical studies have been conducted.[3] These experimental and theoretical results suggest that small clusters have compact and highly coordinated structures, which are completely different from the bulk diamond lattice. Several groups have investigated the growth of electronic level structure of semiconductor clusters with using the photoelectron spectroscopy of negatively-charged Si_n^-, Ge_n^-, and Sn_n^- cluster.[4-7] Ionization potentials (IPs) are also important to understand the electronic structure and stability of clusters. In our previous papers,[8] we have reported the photoionization thresholds of Si_n (n=2-200) examined with a wide photoionization energy (5.0-8.5 eV). The IPs have found to exhibit a large gap in between n=20 and 22. This gap has been tentatively ascribed to the structural transition of neutral silicon clusters in analogy with that for the cluster ions observed in the mobility measurements.[3]

In the present work, we examine the photoionization thresholds of Ge_n (n=2-57) and Sn_n (n=2-41) clusters in the energy region of (5.0-8.8 eV) to obtain further information on the size dependence of IPs for semiconductor clusters. In the energy region above 6.42 eV (ArF laser), high-output vacuum ultraviolet (VUV) laser light generated by anti-Stokes (AS) conversion is used as the photoionization light source to bracket the IPs. We also study the photodissociation processes of the positive charged tin clusters to obtain information on the stabilities and structures of these clusters.

Experimental

The germanium and tin clusters are produced with a laser vaporization source. The second harmonic of a pulsed Nd:YAG laser is focused onto the surface of the sample rod, which is rotated and translated within an aluminum source block. Germanium (or tin) atoms evaporated from the rod surface are mixed with He buffer gas and flowed into a cylindrical flow tube, where cooling and cluster growth occur. This tube is maintained at ca. 80 K to produce the cold clusters. Clusters thus produced are collimated with a skimmer and introduced to the ion extraction region of a time-of-flight (TOF) mass spectrometer, where the clusters are photoionized. Cluster ions are introduced to the reflectron TOF mass spectrometer and detected by microchannel plates.

A high-output VUV laser is used in the energy region above 6.42 eV as the photoionization light source. The VUV light is generated by an anti-Stokes (AS) conversion of narrow-bandwidth UV radiation at 193, 248, and 266 nm. For example, in the photoionization experiment with the AS conversion at 248 nm, the frequency doubled output of a Nd:YAG-laser pumped dye laser is amplified by a KrF excimer laser. The amplified 248-nm laser light (10 mJ/pulse) is focused into a Raman shifter filled with 12-atm H_2 gas. The radiation leaving the Raman shifter is dispersed by a rotatable CaF_2 prism and is introduced to the ionization region through an evacuated tube. Thus, the VUV

radiations in the energy region 6.43-8.79 eV are generated with an energy interval less than 0.22 eV. The ionization laser fluence is attenuated as low as possible to avoid multiphoton ionization and photodissociation processes. For the photoionization experiment in the energy region below 6.42 eV, the second harmonic of an excimer-laser pumped dye laser and the sum frequency of a frequency-doubled OPO laser and the fundamental of the Nd:YAG laser are used as the light sources.

Photodissociation experiments for the positively charged tin clusters are conducted with the reflectron TOF mass spectrometer. The Sn_n^+ ions produced by the laser vaporization method are accelerated colinearly with the incident cluster ion beam by pulsed electric fields in the extraction region of mass spectrometer. The cluster ions of a given mass to charge ratio are irradiated with a photolysis laser at the entrance of the ion reflector. Photofragment ions are mass analyzed in the reflectron and detected by microchannel plates. The 4th harmonic of Nd:YAG laser (4.66 eV) is used as the photolysis light.

Results and Discussion

Figure 1 shows the typical TOF mass spectra of Ge_n^+ (n=2-30) clusters measured at various photon energy in the VUV region. As shown in Fig. 1a, all clusters with $n \leqq 10$, except for n=8, are not observed at 7.06 eV (248 AS-4). With an increase of photon energy, the ion signals of Ge_n^+ (n=6, 7, 9, and 10) increase rapidly as shown in Fig. 1b, 1c, and 1d. As in the case of Si_n, Ge_n have known to exhibit a fission-type fragmentation.[2] This process disturbs an accurate determination of the photoionization thresholds as described in our previous paper for silicon clusters.[8] However, the analysis of these mass spectra as well as the careful examination of the relative intensity of these ions to those for Ge_{22-30} in the mass spectra produced at several ionization energies allows 7.58-7.76 eV to be placed on the IPs of Ge_6, Ge_7, and Ge_{10}. As shown in Fig. 1e, we observe the weak ion signals of Ge_n^+ with n=2-5 at 8.09-eV (248 AS-4). The relative intensities of these ions do not change appreciably even in the mass spectrum recorded with the highest-energy VUV light (8.79 eV, 266 AS-8). Thus these results may indicate that the abundance of the clusters with n=2-5 in the molecular beam are relatively low and the IPs of these clusters are lower than 8.09 eV. The similar trend has also been reported for tin and lead clusters.[9] With a careful analysis of the mass spectra, we determine the IPs of Ge_2, Ge_3, Ge_4, and Ge_5 as 7.58-7.76, 7.97-8.09, 7.87-7.97, and 7.87-7.97 eV, respectively. The ionization thresholds of Ge_n (n=11-18) are also determine with the photoionization laser in the energy region of 6.43-7.06 eV. For Ge_{17}, we cannot determine the IP definitively, because of its low abundance in the molecular beam (see Fig. 1). We also examine the photoionization process and photoionization thresholds of tin clusters using the same technique. The ionization potentials of Ge_n (n=2-57) and Sn_n (n=2-41) determined in the present studies are summarized in Figs. 2a and 2b, respectively[10]: The IPs are plotted against $n^{-1/3}$, which is based on a classical conducting spherical droplet (CSD) model. In the figures, the IPs calculated using the CSD model are also presented by solid lines.

As it is clearly seen in Figs. 2a and 2b, the size dependence of the IPs for Ge_n and Sn_n ($n \leqq 11$) is very similar to each other. The IPs for Ge_2 and Sn_2 are slightly

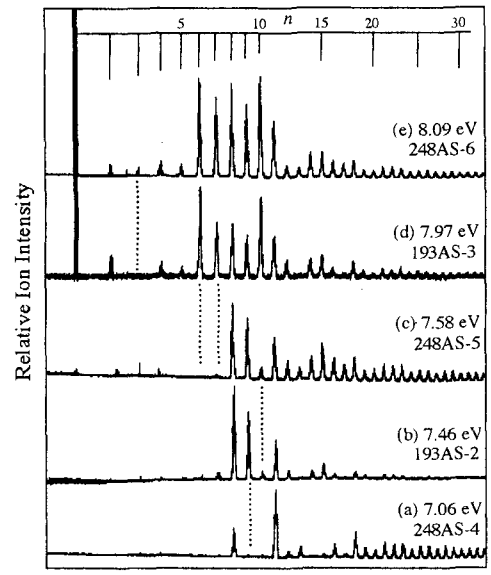

Fig. 1. A series of germanium cluster photoionization mass spectra taken at the indicated energies; (a), (c), and (e) correspond to the AS-4, AS-5, and AS-6 lines of the 248-nm radiation, respectively, while (b) and (d) correspond to the AS-2 and AS-3 lines of 193-nm radiation, respectively.

lower than the atom itself (7.88 and 7.43 eV for Ge and Sn, respectively) and they become higher for n =3-5. IPs of Ge_n and Sn_n with n=6 and 7 are found to be rather high, while those of both Ge_8 and Sn_8 are much lower than its neighbors. The rather high IPs of n=6 and 7 are consistent with the theoretical calculations, which predict the stable closed-shell structure of these clusters. The photoelectron spectroscopy studies on Ge_n^- and Sn_n^- also strongly support the special stability of these clusters.[4-7] The rapid decrease in IP from n=7 to 8 has also been observed for Si_8, though the amount of reduction is smaller than those of Ge_8 and Sn_8. For tin clusters, the large decrease in IP and binding energy for n=8 have been reproduced by the calculations[11] and explained by a drastic reduction of the HOMO-LUMO gap between n=7 and n=8, which is caused by a loss of symmetry. The other remarkable features in the IP plots shown in Fig. 2 are the substantially high IPs of Ge_{10} and Sn_{10}. These results seem to indicate that Ge_{10} and Sn_{10} are more stable than its neighbors as predicted by the theoretical calculations.[11] The higher peak-intensity of Ge_{10}^+ in the mass spectra recorded with the photoionization energy much higher than its IPs (see Fig. 1e), suggesting the higher abundance of this cluster in the molecular beam, is consistent with the above conclusions. These trends in IPs for small Ge_n and Sn_n clusters have also been observed for Si_n.[8] Therefore, the present results as well as the theoretical results in literatures indicate that Si_n, Ge_n, and Sn_n clusters with less than 11 atoms may have similar electronic and geometrical structures.

As shown in Fig. 2, the size dependence for the IPs of

medium size Ge_n and Sn_n is found to be completely different. For Ge_n, the IPs decrease rapidly from n=16 to

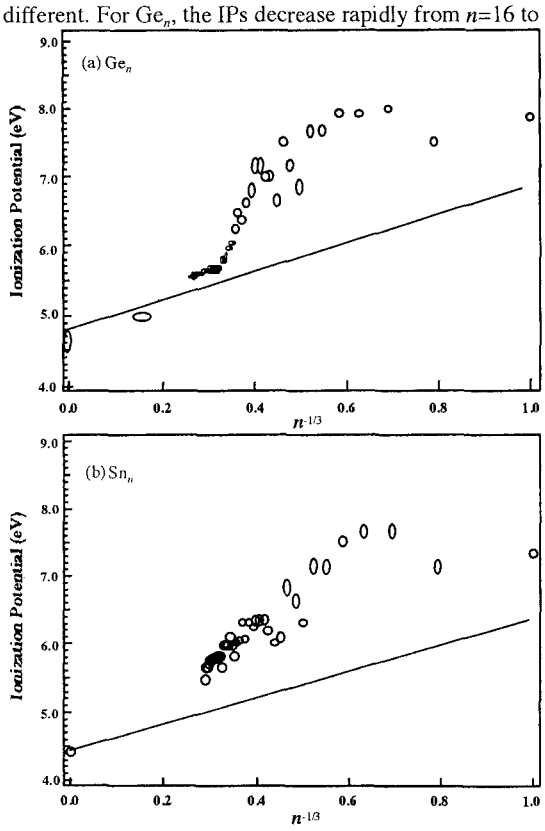

Fig. 2. Ionization potentials of (a) Ge_n (n=2-57) and (b) Sn_n (n=2-41) plotted versus $n^{-1/3}$. The solid lines represent the prediction of the spherical droplet model with the reported bulk work functions.

n=26 and do not follow the CSD model (a solid line shown in Fig. 2a). For large germanium clusters (n>27), the IPs decrease gradually to near bulk work function (4.80 eV) with increasing cluster size. This feature in the size dependence of IPs for Ge_n is very similar to that found for Si_n in the previous work: a large gap in IP (ca. 1.5 eV) between Si_{20} and Si_{22} has been observed.[8] The rapid decrease in the observed IPs for Si_n and Ge_n at n~20 atoms clearly indicates an extensive change in the electronic structure of these clusters in this size regime probably induced by a geometrical change.

According to the experimental and theoretical studies,[3] small Si_n and Ge_n clusters with less than 10 atoms have highly coordinated compact structures, which are completely different from those of their bulk solid: diamond lattice structure with tetrahedral bonding. Thus a structural transition from the compact molecular structure to the bulk-like one is expected to occur with increasing n. Until now, many theoretical efforts have been made to estimate the critical size of this transition.[12-14] However, all theoretical calculations include, to some extent, an extrapolation to evaluate the critical size and their predicted numbers are widely dispersed (n=17-4000). Experimental efforts to explore the critical size of the structural transition have also been made.[3,8] As mentioned previously, Jarrold and coworkers have examined the mobilities of size-selected Si_n^+ cluster ions using injecting-ion drift-tube techniques.[3] They have found that the clusters with $10 \le n \le 34$ are considered to follow a prolate growth sequence, while large clusters ($n \ge 24$) have more spherical geometry and both isomers coexist over the size range of $24 \le n \le 34$. The results suggest a structural transition for clusters with ~27 atoms. The observed structural transition has been assigned to that from geometries with the atoms arranged on a single shell to those with the atoms arranged in two shells. Since the positively charged clusters are produced by removing an electron from a nonbonding orbital, we can also expect the existence of the structural isomers for neutral clusters. Thus, in our previous paper,[8] we have discussed the large IP gap of Si_n in terms of the structural transition similar to that found for Si_n^+. Similarity in size dependence of IPs for Si_n^+ and Ge_n^+ found in the present study also suggests the existence of the similar transition for Ge_n^+. Jarrold and coworkers[3] have also investigated the mobilities of Ge_n^+ (n=7-54), and observed a prolate growth for Ge_n^+ with n=10-35 and a gradual deviation from this growth sequence for n>35. However, they have not observed a structural transition for Ge_n^+ with n=7-50, except for Ge_{40}^+. These observations for Ge_n^+ are rather unexpected when compared with the present results on IPs for Ge_n clusters. Without elaborate theoretical calculations on the geometrical and electronic structures of Ge_n (n>20), it is difficult to comment on the difference in the features for those germanium clusters observed in the mobility and photoionization experiments.

As mentioned previously, the size dependence of IPs for small tin clusters is very similar to those for Si_n and Ge_n clusters. However, medium size Sn_n clusters exhibit a quite different trend. The IPs decrease gradually without an appreciable gap and seem to follow the CSD model as shown in Fig. 2b. On the other hand, Jarrold and coworkers have examined the mobilities of Sn_n^+ up to n=68 using the same technique and found no abrupt structural transition as observed for Si_n^+.[3] They have found that tin clusters track the prolate growth pattern found for Si_n^+ and Ge_n^+ up to n~35 and gradually rearrange towards near spherical geometries in the n~35–65. To explain the results on the mobilities for Sn_n^+, these authors have pointed out a possible bonding rearrangement of Sn_n^+ to the compact ball expected for metal nanoparticles. These experimental results on the IPs and mobilities for tin clusters seem to be related to its bulk properties. In solid, tin has properties intermediate to those of germanium and lead: diamond structure (α-tin) as in the cases of Si and Ge at low temperature, but the structure of tin transforms at T>287 K into metallic phase (β-tin) with a body-centered tetragonal structure. Taking into account the monotonic decrease in IPs seen in Fig. 2, as well as the mobility results and the bulk properties of tin, the clusters with $n \ge 10$ are considered to grow with maintaining the compact metallic-like structure similar to those for the small clusters.

As shown in Fig. 2, the size dependence of the IPs for Sn_n^+ starts deviating from those for Si_n^+ and Ge_n^+ at n~13. These changes may also reflect on the structure and stabilities of the Sn_n^+ clusters. In order to get further insight into the properties of these clusters, we examine

the photodissociation processes of mass-selected tin clusters with the reflectron TOF mass spectrometer. We

Table 1. Photodissociation products of Si_n^+, Ge_n^+, and Sn_n^+ cluster cations at 266 nm

n	Products Si_m^+ of Si_n^+ (a)	Products Ge_m^+ of Ge_n^+ (a)	Products Sn_m^+ of Sn_n^+
5			**4**, 3, 2
6			**5**, **4**, weaker 3, 2
7			6, 5, 4, 3
8			**7**, **6**, 5, 4
9			**7**, weaker 4, 5, 6, 8
10	**6**, 4, 7, 5	6, 7, 4, 8, 9, 5	**8**, 9, 7, 6, 5, 4
11	7, 6, 5, 4, 10	7, 6, 5, 10, 4	**10**, 7, 6, 9, 8, 5, 4
12	**6**	**6**, 7, 8, 10, 11	**7**, **6**, 8, 10, 11, 9, 5
13	**7**, **6**, 12	6, 7, 3, weaker 11, 12	**7**, **6**, 9, 8, 10, 5, 11
14	7, 8, 10, 6	7, 8, 6, 9	**7**, 8, 6, 10, 9
15	8, 9	**8**, 9, 10	**8**, 7, 9, 10

(a) cited from ref. 2.

use the 4th harmonic of YAG laser at 266 nm (4.66 eV) as the photolysis light. Table 1 lists the photofragmentation product channels of Sn_n^+ (n=5-15) found in the present work. We also list the results on Si_n^+ and Ge_n^+ (n=10–15) reported by Smalley' group.[2] As seen in the Table 1, tin cluster ions exhibit the extensive fission-type fragmentation. The favored products in the photodissociation of Sn_n^+ are also similar to those for Si_n^+ and Ge_n^+. The results are consistent with the arguments on the IP of small clusters mentioned previously; small silicon, germanium, and tin clusters may have the similar electronic and geometrical structures. However, a closer inspection of the table indicates that there exist more fragmentation channels for Sn_n^+ than for Si_n^+ and Ge_n^+. For example, Sn_m^+ with m=5 and 8-11 are observed in the photofragmentation of Sn_{12}^+ in addition to the major favorable fragment ions such as Sn_m^+ (m=6 and 7). On the other hand, Si_{12}^+ produces only Si_6^+ and neutral Si_6 cluster through the fission-type fragmentation. The difference in the photodissociation channel is also clearly seen in the products of Sn_{10}^+: both Si_{10}^+ and Ge_{10}^+ produce the stable cluster ions with 6 atoms, while the favored product of Sn_{10}^+ is the less stable Sn_8^+. These results indicate that the evaporation of atom and/or dimer from Sn_n^+ occurs in addition to the fission-type fragmentation. The former process is usually observed for metal clusters such as Fe_n^+. Therefore, this observation may indicate the metallic-like property of tin clusters and is consistent with the above mentioned IP results. At present, the photodissociation data of Sn_n^+ are limited for small clusters. We are conducting the photodissociation experiments for large tin clusters to confirm these discussions.

Acknowledgment

This work was partially supported by Grants-in-Aid from the Ministry of Education, Science, Sports and Culture of Japan and a JSPS research grant for the Future Program. We are also grateful to the Aichi Science and Technology Foundation for financial supports.

References

1. L. A. Bloomfield, R. R. Freeman, and W. L. Brown, Phys. Rev. Lett. **54**, 2246 (1985).
2. Q. -L. Zhang, Y. Liu, R. F. Curl, F. K. Tittel, and R. E. Smalley, J. Chem. Phys. **88**, 1670 (1988).
3. A. A. Shvartsburg and M. F. Jarrold, Phys. Rev. **B60**, 1235 (1999) and references cited therein.
4. O. Cheshnovsky, S. H. Yang, C. L. Pettiette, M. J. Craycraft, Y. Liu, and R. E. Smalley, Chem. Phys. Lett. **138**, 119 (1987).
5. G. Ganteför, M. Gausa, K. H. Meiwes-Broer, and H. O. Lutz, Z. Phys. **D12**, 405 (1989).
6. G. R. Burton, C. Xu, C. C. Arnold, and D. M. Neumark, J. Chem. Phys. **104**, 2757 (1996).
7. H. Kawamata, Y. Negishi, R. Kishi, S. Iwata, M. Gomei, A. Nakajima, and K. Kaya, J. Chem. Phys. **105**, 5369 (1996).
8. K. Fuke, K. Tsukamoto, and F. Misaizu, Z. Phys. **D26**, S204 (1993); K. Fuke, K. Tsukamoto, F. Misaizu, and M. Sanekata, J. Chem. Phys. **99**, 7805 (1993).
9. K. LaiHing, R. G. Wheeler, W. L. Wilson, and M. A. Duncan, J. Chem. Phys. **87**, 3401 (1987).
10. S. Yoshida and K. Fuke, J. Chem. Phys. **111**, 3880 (1999).
11. B. Wang, L. M. Molina, M. J. L¢pez, A. Rubio, J. A. Alonso, and M. J. Stott, Ann. Phys. **7**, 107 (1998).
12. C. H. Patterson and R. P. Messmer, Phys. Rev. **B42**, 7530 (1990).
13. J. R. Chelikowsky, Phys. Rev. Lett. **60**, 2669 (1988).
14. D. Tomanek and M. Schüter, Phys. Rev. Lett. **56**, 1055 (1986).
15. R. Bismas and D. Hamann, Phys. Rev. **B34**, 895 (1986).

(Received December 17, 1999; Accepted August 31, 2000)